BLADE DYNAMICS IN ORTHOGONAL WAVE-CURRENT CONDITIONS

Zichen Xu, National University of Singapore, zichen_xu@u.nus.edu
Jiarui Lei, National University of Singapore, jlei@nus.edu.sg

INTRODUCTION

Aquatic vegetation provides various ecosystem services (Barbier et al., 2011). It supports biodiversity by providing habitats and shelter areas for various fisheries (Costanza et al., n.d.) and supplying food for larger herbivorous animals such as the dugong and green turtles (Waycott et al., 2005). Acting as a carbon sink, aquatic vegetation sequesters a greater amount of carbon per hectare per year than rainforest (Fourqurean et al., 2012). Shoreline vegetation attenuates incoming waves and protects shorelines from erosion due to wave impact (e.g., Barbier et al., 2011; Koch et al., 2009). Wave dissipation over aquatic vegetation has long been noted. Researchers have developed site- and species-specific models to describe wave damping over artificial vegetation and natural habitats (e.g., Möller et al., 2014; Smallegan et al., 2016). Because aquatic vegetation plays such an important role in these processes, it is recognized as a promising nature-based solution for coastal protection. Evaluating and understanding nature-based solutions requires knowledge of the dynamics of aquatic vegetation under coastal flows.

Flexible vegetation reconfigures with flows and behaves differently from rigid vegetation, thus leading to different wave-damping models. Under unidirectional currents, flexible vegetation bends in the same direction as currents, while under waves, the tip of flexible vegetation follows the motion of water. The motion of flexible vegetation leads to the reduction of frontal area and the relative velocity between vegetation and flows, thus leading to the decrease of drag force that acts on flows. To address the change of drag force, Losada et al. (2016) applied deflected height, l_D, based on plant bending angle (θ) to account for the impact from the reduction in drag-forming area. However, reconfiguration of flexible vegetation induced by flow causes a reduced drag force due to both the decrease in the frontal area and more streamlined shapes of bending blades. Luhar and Nepf, (2011) addressed the importance of both frontal area and streamlined shape with effective blade length (l_e). Since there is no evidence mentioned that reduction in the frontal area dominated drag force reduction, overestimation of wave dissipation can be caused because l_D is larger than l_e. Lei and Nepf (2019b) then applied l_e to flexible seagrass studies and proposed theoretical scaling laws to predict wave decay over a meadow of flexible vegetation. The framework of l_e was then be extended to co-directional wave-current studies, and the blade motion was found to be dependent on current-to-wave velocity ratio (Lei & Nepf, 2019a). Schaefer and Nepf (2022) evaluated the work by wave attenuation experiments over a flexible seagrass model under co-directional wave-current flows. To date, vegetation dynamics under orthogonal wave-current conditions (i.e., the current is perpendicular to the direction of wave propagation), which usually correspond to wave-induced longshore currents near the coast, have not yet emerged.

OBJECTIVES AND SCOPES

The focus of this study is to address the scientific challenge of understanding the behavior of flexible vegetation, considering orthogonal wave-current conditions. Our research enhances the existing body of work through several novel contributions.

I. Conducting direct measurement of the drag force of a single flexible blade to modify the coefficients of the scaling law of l_e under orthogonal wave-current conditions.
II. Developing and validating the scaling laws for l_e under orthogonal wave-current conditions.
III. Extending the new scaling laws to predict wave damping over a meadow of flexible vegetation under orthogonal wave-current conditions

THEORETICAL BACKGROUND AND HYPOTHESISES

To describe the dynamics of flexible blades, we use the effective blade length, l_e, defined as the length of a rigid blade that experiences the same drag force as a flexible blade of length l. Two dimensionless parameters are used to describe the blade's effective length in pure currents, pure waves, and co-directional waves and currents (e.g., Lei & Nepf, 2019b; Luhar & Nepf, 2011). The Cauchy number (Ca) is the ratio of hydrodynamic drag to the restoring force due to blade stiffness. The blade length ratio, L, is the ratio of blade length, l, to wave excursion, A_w.

$$Ca = \frac{\frac{1}{2} C_D \rho w_b U^3 l^3}{EI} \tag{1}$$

$$L = \frac{l}{A_w} = \frac{2\pi l}{U_w T} \tag{2}$$

Here, w_b is the blade width, ρ is the density of water, U is the relative velocity between vegetation and flow, l is the blade length, E is the Young's modulus, U_w is the magnitude of horizontal wave velocity and $I = w_b t_b^3/12$ is the bending moment of inertia with t_b the blade thickness. Lei & Nepf (2019b) suggest the following equations to estimate l_e in co-directional waves and currents.

$$\begin{cases} U_c < 0.25\, U_w, & \frac{l_e}{l} = (1.09 \pm 0.07)(Ca_w L)^{-0.25 \pm 0.02} \\ 0.25\, U_w \le U_c < 2U_w, & \frac{l_e}{l} = 0.9 {Ca_{wc}}^{-1/3} \\ U_c \ge 2U_w, & \frac{l_e}{l} = 0.9 {Ca_c}^{-1/3} \end{cases} \tag{3}$$

where the subscripts w, c, and wc denote the pure-wave, pure-current, and co-directional wave-current conditions, respectively.

In our current study, we focus on orthogonal wave-current conditions. The following is a hypothesis for how the impact of orthogonal currents might be captured in the effective blade length framework, using the dimensionless parameters Ca, and current-to-wave ratio U_c/U_w. We caution that blade twisting (torsion) has not been taken into consideration at this stage.

Regime 1: Weak Waves and Current ($Ca_c < 1, Ca_w < 1$). During this phase, the vegetation experiences minimal movement, and the effective blade length closely matches the actual blade length, denoted as $l_e \sim l$.
Regime 2: Weak current ($u_c \ll u_w, Ca_c < 1, Ca_w > 1$). The current's influence on blade dynamics is negligible. The effective length can be quantified as it is in the pure wave conditions.
Regime 3: Intermediate current ($u_c/u_w \sim 1, Ca_c > 1, Ca_w > 1$). The current results in a mean deflection of the blade perpendicular to the wave propagation direction. The drag force induced by the current strives to extend the blade, consequently increasing l_e by opposing the motion of the blade.
Regime 4: Strong current ($u_c \gg u_w, Ca_c > 1, Ca_w > 1$). The blade becomes fixed in a deflected position due to the robust current. As the blade is nearly perpendicular to the wave propagation direction, the anticipated effective blade length in the wave propagation direction approximates l.

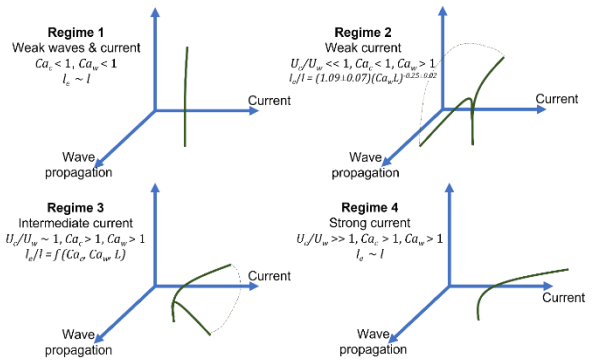

Figure 1 – Proposed scaling laws for l_e under different orthogonal wave-current regimes using the dimensionless parameters Ca_c (current Cauchy number), Ca_w (wave Cauchy number), L (blade length ratio), and U_c/U_w (current-to-wave ratio). The directions of waves and currents are denoted by blue arrows. Dashed lines denote the range of motion of the blade tip.

EXPERIMENTAL METHODS

The experiments were conducted in the proposed 4 regimes. All laboratory experiments were carried out in a 24m-long, 10m-wide, and 0.9m-deep wave basin. For simplicity, EPDM rubber rods were used as the representative of flexible vegetation. Two individual vegetation shoots were attached to two submersible force transducers (FUTEK LSB210 with a 50ft cable length and 2lbs capacity), which are fixed at a customized pyramid in directions that are perpendicular to each other. The drag force at wave propagation and current direction was measured for three minutes at a sampling rate of 300 Hz. At the same time as force measurements, surface displacement and flow velocities were also measured by wave gauges and ADV. The normalized effective length (l_e/l) is determined by comparing the measured drag force with the force measured on a rigid reference shoot of identical geometry to the original length. The relationship between l_e/l and the dimensionless parameters, Ca_c (current Cauchy number), Ca_w (wave Cauchy number), L (blade length ratio) and u_c/u_w (current-to-wave ratio) were developed.

REFERENCES

Barbier, E. B., Hacker, S. D., Kennedy, C., Koch, E. W., Stier, A. C., & Silliman, B. R. (2011). The value of estuarine and coastal ecosystem services. *Ecological Monographs*, *81*(2).

Beth Schaefer, R., & Nepf, H. (2022). Wave damping by seagrass meadows in combined wave-current conditions. *Limnology and Oceanography*, *67*(7), 1554–1565. https://doi.org/10.1002/lno.12102

Costanza, R., Hannon, B., Limburg, K., Naeem, S., O'Neill, R. V., Raskin, R. G., & Sutton, P. (n.d.). *The Value of the World's Ecosystem Services and Natural Capital*.

Fourqurean, J. W., Duarte, C. M., Kennedy, H., Marbà, N., Holmer, M., Mateo, M. A., Apostolaki, E. T., Kendrick, G. A., Krause-Jensen, D., McGlathery, K. J., & Serrano, O. (2012). Seagrass ecosystems as a globally significant carbon stock. *Nature Geoscience*, *5*(7), 505–509. https://doi.org/10.1038/ngeo1477

Koch, E. W., Barbier, E. B., Silliman, B. R., Reed, D. J., Perillo, G. M., Hacker, S. D., Granek, E. F., Primavera, J. H., Muthiga, N., Polasky, S., Halpern, B. S., Kennedy, C. J., Kappel, C. V., & Wolanski, E. (2009). Non-linearity in ecosystem services: Temporal and spatial variability in coastal protection. *Frontiers in Ecology and the Environment*, *7*(1), 29–37. https://doi.org/10.1890/080126

Lei, J., & Nepf, H. (2019a). Blade dynamics in combined waves and current. *Journal of Fluids and Structures*, *87*, 137–149. https://doi.org/10.1016/j.jfluidstructs.2019.03.020

Lei, J., & Nepf, H. (2019b). Wave damping by flexible vegetation: Connecting individual blade dynamics to the meadow scale. *Coastal Engineering*, *147*, 138–148. https://doi.org/10.1016/j.coastaleng.2019.01.008

Losada, I. J., Maza, M., & Lara, J. L. (2016). A new formulation for vegetation-induced damping under combined waves and currents. *Coastal Engineering*, *107*, 1–13. https://doi.org/10.1016/j.coastaleng.2015.09.011

Luhar, M., & Nepf, H. M. (2011). Flow-induced reconfiguration of buoyant and flexible aquatic vegetation. *Limnology and Oceanography*, *56*(6), 2003–2017. https://doi.org/10.4319/lo.2011.56.6.2003

Möller, I., Kudella, M., Rupprecht, F., Spencer, T., Paul, M., Van Wesenbeeck, B. K., Wolters, G., Jensen, K., Bouma, T. J., Miranda-Lange, M., & Schimmels, S. (2014). Wave attenuation over coastal salt marshes under storm surge conditions. *Nature Geoscience*, *7*(10), 727–731. https://doi.org/10.1038/ngeo2251

Smallegan, S. M., Irish, J. L., Van Dongeren, A. R., & Den Bieman, J. P. (2016). Morphological response of a sandy barrier island with a buried seawall during Hurricane Sandy. *Coastal Engineering*, *110*, 102–110. https://doi.org/10.1016/j.coastaleng.2016.01.005

Waycott, M., Longstaff, B. J., & Mellors, J. (2005). Seagrass population dynamics and water quality in the Great Barrier Reef region: A review and future research directions. *Marine Pollution Bulletin*.